Weierstraß-Institut
für Angewandte Analysis und Stochastik

Generation of terahertz radiation from ionizing two-color laser pulses in Ar filled metallic hollow waveguides

I. Babushkin[1], S. Skupin[2], and J. Herrmann[3]

[1]   Weierstrass Institute for Applied Analysis and Stochastics, Mohrenstr. 39, 10117, Berlin, Germany,
      E-mail: babushkin@wias-berlin.de
[2]   Max Planck Institute for the Physics of Complex Systems, Nöthnitzer Str. 38, 01187 Dresden, Germany;
      Friedrich Schiller University, Institute of Condensed Matter Theory and Optics,
      Fröbelstieg 1, 07742 Jena, Germany.

[3]   Max Born Institute for Nonlinear Optics and Short Pulse Spectroscopy, Max-Born-Str. 2A, 12489,
      Berlin, Germany.

Abstract

The generation of THz radiation from ionizing two-color femtosecond pulses propagating in metallic hollow waveguides filled with Ar is numerically studied. We observe a strong reshaping of the low-frequency part of the spectrum. Namely, after several millimeters of propagation the spectrum is extended from hundreds of GHz up to ~ 150 THz. For longer propagation distances, nearly single-cycle near-infrared pulses with wavelengths around 4.5 μm are obtained by appropriate spectral filtering, with an efficiency of up to 0.25 %.

1   Introduction

In recent years, the range of wavelengths where coherent radiation can be generated has grown dramatically into both high and low frequency domain. Remarkably, most of the methods to obtain radiation at extreme frequencies use, in one or the other way, nonlinear processes in laser-induced plasma. One prominent example is high harmonic generation (HHG) where frequencies thousand times larger than the frequency of the pump pulse are excited, exploiting the recollision dynamics of electrons ionized by the intense light pulses. More recently it was demonstrated that a two-color fs beam allows generation of new frequencies just in the opposite part of the spectrum, namely in the THz range, hundreds times smaller than the optical pump frequency. To this end, a short two-color pulse of fundamental frequency and second harmonic is strongly focused into a plasma spot [1–12] The observed THz emission generated in this scheme has been attributed to the laser-induced plasma current in the asymmetric two-color field [7,8]. Using such scheme generation of strong THz radiation was reported, with a spectrum which can be as broad as 70 THz [8]. Such broad-band coherent radiation can allow new applications providing the possibility to probe complex molecules or as an analytical and imaging tool in a broad range of fields.

In this article we consider a modification of the above described focusing geometry in a bulk gas by using a metallic hollow waveguide with a cladding from aluminum to guide both THz and optical radiation. The use of a waveguide prevents the diffraction of light for all wavelengths involved. In addition, such setup allows to realize nearly single-mode operation for a wide range of frequencies. High threshold intensities for ionization-induced processes in the range larger than 100 TW/cm^2 have been already realized in the context of HHG schemes in hollow waveguides [13, 14]. We will show that during propagation a dramatic spectral broadening of the low-frequency part of the spectrum occurs, caused by only modest changes in

the fundamental and second harmonic fields. In particular, ultrashort pulses of 10 fs duration lead to the formation of low-frequency spectrum extended from several hundreds of GHz to approximately 150 THz. Upon further propagation we report the generation of nearly single-cycle pulses with central wavelengths around 4.5 μm and efficiency of the order of 0.25 %.

2   The model

In the previous works, THz emission by two-color fields in gases has been interpreted by four-wave mixing rectification [1–5]. In contrast, later studies attributed THz emission to the laser-induced plasma-current in the asymmetric two-color field [7–12] described by the local quasi-classical model of the electron current in the laser field without taking into account propagation effects. As an alternative approach, particle-in-cell simulations were used [9, 10]. Those methods are, however, computationally very expensive, and propagation effects have been taken into account over distances of a few micrometers only. In such models the microscopic current is described as a sum over contributions from all electrons, born at discrete times t_n. The "continuous" analog of this approach is given by ([7, 8, 11])

$$\mathbf{J}(t) = q \int_{-\infty}^{t} \mathbf{v}(t, t_0)\dot{\rho}(t_0)dt_0, \tag{1}$$

where q is the electron charge. The current density $\mathbf{J}(t)$ at the time t is obtained by integrating over all impacts from different ionization times t_0: $\mathbf{v}(t, t_0)$ is the velocity of electrons at time t which were born at time t_0, and $\delta\rho(t_0) = \rho(t_0 + \delta t) - \rho(t_0) \approx \dot{\rho}(t_0)\delta t$ is the density of electrons born at time t_0 [1]. This approach was utilized in the previous works of Kim and coauthors [7, 8, 11].

The additional integration over the variable t_0 increases the numerical effort, but one can eliminate the microscopic velocity distribution $\mathbf{v}(t, t_0)$ and derive a differential equation for the macroscopic current density $\mathbf{J}(t)$. Assuming no interaction with other particles and zero velocity of new-born electrons, the equation for the electron velocity can be written as $\mathbf{v}(t, t_0) = \frac{q}{m_e} \int_{t_0}^{t} \mathbf{E}(\tau)d\tau$ (where $\mathbf{E}$ is the electric field, m_e is the electron mass). With the simple additive property of integrals we can rewrite it as $\mathbf{v}(t, t_0) = \mathbf{v}(t, -\infty) - \mathbf{v}(t_0, -\infty)$. Substituting this into Eq. (1) and differentiating with respect to t we obtain $\dot{\mathbf{J}}(t) = q\dot{\mathbf{v}}(t)\rho(t)$. It is easy to see that by introducing new variables $\mathbf{v}' = \mathbf{v}\exp(-\nu_e t)$, $\mathbf{J}' = \mathbf{J}\exp(-\nu_e t)$ (where ν_e is the electron-ion collision rate) and proceeding analogously we can include collisional effects as well, and finally obtain

$$\dot{\mathbf{J}}(t) + \nu_e \mathbf{J}(t) = \frac{q^2}{m_e}\mathbf{E}(t)\rho(t). \tag{2}$$

---

[1]We use the convention $\dot{f} \equiv \frac{\partial f}{\partial t}$.

Indeed, Eq. (2) coincides with the well known (and very commonly used) equation for the current in plasmas [15, 16].

In the present article, the static model for the tunneling ionization [17] is used:

$$\dot{\rho}(t) = W_{\text{ST}}[E(t)][\rho_{\text{at}} - \rho(t)], \qquad W_{ST}[E(t)] = \alpha \frac{E_a}{E(t)} \exp\left\{-\beta \frac{E_a}{E(t)}\right\}. \qquad (3)$$

Here, ρ_{at} is the neutral atomic density, and $E_a \approx 5.14 \times 10^{11}$ Vm^{-1} the atomic field; the coefficients $\alpha = 4\omega_a r_H^{5/2}$ and $\beta = (2/3)r_H^{3/2}$ are defined through the ratio of ionization potentials of argon and hydrogen atoms $r_H = U_{Ar}/U_H$, $U_{Ar} = 15.6$ eV, $U_H = 13.6$ eV, and $\omega_a \approx 4.13 \times 10^{16}$ s^{-1} [6, 17].

To describe the light propagation, we use the so called forward Maxwell equation (FME) for the fast oscillating optical field $\mathbf{E}(\mathbf{r}, z, t)$ in the waveguide with the optical axis along z direction [18]:

$$\frac{\partial \tilde{\mathbf{E}}(\mathbf{r}, z, \omega)}{\partial z} = ik(\omega)\tilde{\mathbf{E}}(\mathbf{r}, z, \omega) + \frac{i}{2k(\omega)}\Delta_\perp \tilde{\mathbf{E}}(\mathbf{r}, z, \omega) + \frac{i\mu_0\omega c}{2n(\omega)}\tilde{\mathbf{P}}_{nl}(\mathbf{r}, z, \omega), \qquad (4)$$

where $\mathbf{r} = \{x, y\}$, $\Delta_\perp = \partial_{xx} + \partial_{yy}$, $n(\omega)$ is the refractive index of Ar, $k(\omega) = n(\omega)\omega/c$. $\tilde{\mathbf{E}}(\mathbf{r}, z, \omega)$ and $\tilde{\mathbf{P}}_{nl}(\mathbf{r}, z, \omega)$ are the Fourier transforms of $\mathbf{E}(\mathbf{r}, z, t)$, $\mathbf{P}_{nl}(\mathbf{r}, z, t)$ with respect to time, $\mathbf{P}_{nl}$ is the nonlinear polarization, which includes both the Kerr ($\mathbf{P}_{Kerr} = \varepsilon_0\chi^{(3)}|\mathbf{E}|^2\mathbf{E}$) nonlinearity and the plasma contribution: $\tilde{\mathbf{P}}_{nl} = \tilde{\mathbf{P}}_{Kerr} + i\tilde{\mathbf{J}}/\omega + i\tilde{\mathbf{J}}_{loss}/\omega$, where $\mathbf{J}_{loss} = W_{\text{ST}}(\rho_{\text{at}} - \rho)U_{Ar}/\mathbf{E}$ is a loss term accounting for photon absorption during ionization; "division by a vector" means the component-wise division [17]. Decomposing the field into a series of linear eigenmodes of the waveguide $\{\mathbf{F}_j(\mathbf{r}), j = 1, \dots \infty\}$ with corresponding propagation constants $\beta_j(\omega)$, we obtain the following set of equations for the amplitudes of the eigenmodes E_j, coupled through the nonlinear polarization term $P_{nl}^{(j)} = \int \mathbf{F}_j \mathbf{P}_{nl} d\mathbf{r}$:

$$\frac{\partial \tilde{E}_j(z, \omega)}{\partial z} = i\beta_j(\omega)\tilde{E}_j(z, \omega) + i\frac{c\mu_0\omega^2}{2k(\omega)}\tilde{P}_{nl}^{(j)}(z, \omega). \qquad (5)$$

3 Numerical simulations

In our simulations, we assume a dielectric waveguide with aluminum coating of the inner walls and diameter $d = 100$ μm. Such waveguides can be routinely produced (see, e.g., [19]). The main purpose of the waveguide is not to modify the dispersion relation but to confine both pump and THz radiation (especially the latter, because it quickly spreads out otherwise as a result of diffraction [25]). Taking into account that THz as well as fundamental and second harmonic frequencies undergo strong absorption due to plasma generation a long waveguide is not useful. Therefore, we restrict our simulations to distances ≤ 1 cm.

The linearly-polarized waveguide mode EH$_{11}$ has no cut-off at low frequencies, and the fundamental and second-harmonic frequencies can be coupled into the waveguide
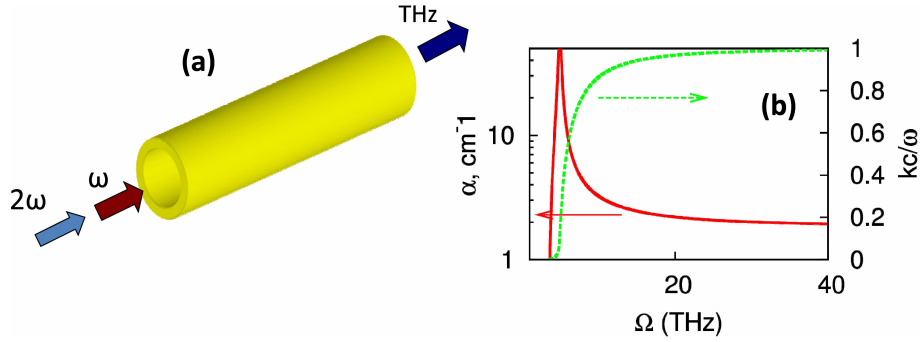
Figure 1: (a) Scheme for THz generation considered in this article. A short pulse with center frequency $\nu_0 = 375$ THz (corresponding to wavelength $\lambda = 800$ nm) and its second harmonic are focused into an aluminum coated hollow waveguide. The THz emission is detected at the exit of the waveguide. (b) Losses α (red solid line) and refractive index change $\delta n = kc/\omega$ (green dashed line) induced by the Al waveguide with the diameter $d = 100$ μm for the mode EH_{11} versus frequency $\Omega = \omega/2\pi$.

with almost 100 % efficiency from the free-space propagating laser mode. The dispersion and losses for the mode EH_{11} of the 100-μm waveguide are shown in Fig. 1(b) in low-frequency range. Both quantities are calculated using the direct solution of the corresponding boundary value problem [20], Drude model for the dispersion in aluminum [21] as well as Sellmeier formula for the dispersion in argon [22]. One can see that the losses are relatively large only in the small frequency range corresponding to wavelengths of the order of the waveguide diameter. The aluminum coating was chosen because then the modeling of linear dispersion and losses in the whole frequency range from sub-THz to sub-PHz is straight forward using the Drude model [21]. In contrast, for dielectric coatings (such as fused silica) such simple description for the whole spectral region of interest fails. Nevertheless, we expect even weaker losses than for the metallic waveguide.

Results from simulations of ultrashort pulses with 10 fs duration and frequencies $\nu_0 = 375$ THz (corresponding to the wavelength $\lambda = 800$ nm) and $2\nu_0$, having intensities $I_\omega = 10^{14}$ W/cm^2 and $I_{2\omega} = 2 \times 10^{13}$ W/cm^2 correspondingly are shown in Fig. 2. We checked that the transverse field distribution consists predominantly of the fundamental and few higher order modes. At the initial stage of propagation, broadband THz radiation is generated from approximately 0.5 THz to 80 THz (see Fig. 2(a) and (b)). With further propagation (up to 2 mm) the low-frequency part of the spectrum grows in the direction to higher frequencies (up to 150 THz). At the same time, the spectral intensity around 10 THz degrades because of the strong losses of the waveguide mode. From 2 mm up to $\sim$ 7 mm the long-wavelength part of the spectrum shifts continuously towards higher frequencies. Finally, starting from 7 mm the spectrum does not change considerably anymore, except for its decrease due to losses. At this propagation distance, the long-wavelength part of the spectrum
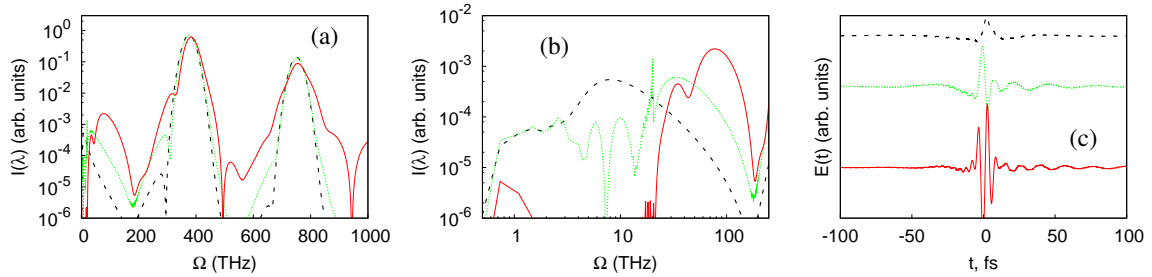
Figure 2: Evolution of the THz spectrum upon propagation for a waveguide with diameter $d = 100$ μm, input intensities $I_\omega = 10^{14}$ W/cm^2, $I_{2\omega} = 2 \times 10^{13}$ W/cm^2 and pulse duration 10 fs. (a) The spectrum and (b) low-frequency part of spectrum (note the logarithmic scale of y-axis in (a) and both axes in (b)) for $z = 0.5$, 2, and 10 mm of propagation (black dashed, green dotted and red solid lines). (c) Pulses obtained by filtering the long-wavelength part of the spectrum below 250 THz. Propagation distances, color coding and line styles are the same as in (a).

is localized around 60-80 THz, with the center around 66 THz (corresponding to a wavelength ~ 4.5 μm). The observed efficiency of this "frequency down-conversion" reaches 0.25 percent.

The electric field obtained by filtering the long-wavelength part of the spectrum for different propagation distances is shown in Fig. 2(c). One can see that despite the strong reshaping of the spectrum, the envelope of the obtained THz pulses does not change significantly. The amplitude of the pulse grows considerably during propagation, from approximately 1 % of the pump amplitude at $z = 0.5$ mm (which correspond to the conversion efficiency $\sim 10^{-4}$) to about 5 % at $z = 10$ mm (which correspond to the conversion efficiency $\sim 2.5 \times 10^{-3}$).

Fig. 2(a) reveals that in contrast to the strong reshaping of the low frequency components, the spectrum in the range of the pump frequencies remains almost unchanged. Nevertheless, the spectrum of the pump broadens slightly upon propagation. Due to plasma-induced refraction index change the maximum frequency of the fundamental pulse is slightly shifted to the blue [23, 24]. In our case the shift is small, only about 10 THz. As elaborated in [25], even small changes in the pump fields can affect dramatically the spectral shape of the generated low-frequency radiation. Such changes affect significantly the temporal positions of the ionization events. Contributions from the electrons born in different ionization events are superimposed, and interference effects lead to a reshaping the THz spectra.

The situation is qualitatively similar for other pulse durations (see Fig. 3). In general, the efficiency of the THz generation is larger for shorter pulse durations (in Fig. 3, spectra are normalized to unity at their maxima, so the efficiencies can be directly compared). This observation can be explained by the additional asymmetry in the current which is introduced by the finite pulse duration and therefore more pronounced for short pulses.
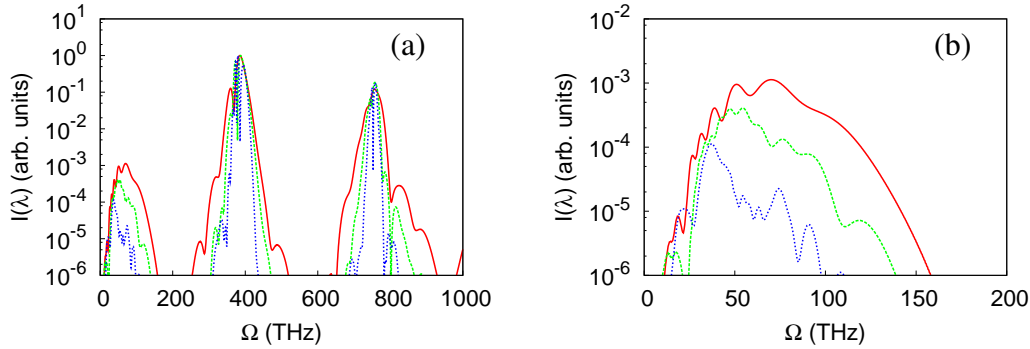
5

Figure 3: Spectra for different input pulse durations (25, 50 and 1000 fs are shown by red solid, green dashed and blue dotted lines, respectively) for 1 cm of propagation. In (a) and (b) the full spectra and their low-frequency parts are shown, respectively. Spectra are normalized to their maximum value, so that efficiencies can be compared.

4   Conclusion

In conclusion, we studied THz generation by plasma currents through noble gas ionization in strong asymmetric laser fields. We have shown that the mechanism allows the relatively simple generation of extremely wide range of frequencies, starting from THz to near infrared. By using hollow waveguides we overcome the strong diffraction of the generated low-frequency generation. We report that depending on the length of the waveguide either THz supercontinuum or almost single-cycle near-infrared pulses can be produced at output with ~ 0.25 % efficiency. We believe that our findings may open new intriguing possibilities to control the spectral and temporal shape of low-frequency radiation generated by the ionization dynamics in intense optical fields.

References

[1] D. J. Cook and R. M. Hochstrasser, "Intense terahertz pulses by four-wave rectification in air," Opt. Lett. **25**, 1210 (2000).

[2] T. Bartel *et al.*, "Generation of single-cycle THz transients with high electric-field amplitudes," Opt. Lett. **30**, 2805 (2005).

[3] X. Xie, J. Dai, and X.-C. Zhang, "Coherent Control of THz Wave Generation in Ambient Air," Phys. Rev. Lett. **96**, 075005 (2006).

[4] J. Dai, X. Xie, and X.-C. Zhang, "Detection of Broadband Terahertz Waves with a Laser-Induced Plasma in Gases," Phys. Rev. Lett. **97**, 103903 (2006).

[5] K. Reimann, Rep. Prog. Phys. "Table-top sources of ultrashort THz pulses," **70**, 1597 (2007).

[6] M. D. Thomson, M. Kreß, T. Löffler, H. G. Roskos, "Broadband THz emission from gas plasmas induced by femtosecond optical pulses: From fundamentals to applications," Laser & Photon. Rev. **1**, 349 (2007).

[7] K.-Y. Kim, J. H. Glownia, A. J. Taylor, and G. Rodriguez, "Terahertz emission from ultrafast ionizing air in symmetry-broken laser fields," Opt. Express **15**, 4577 (2007).

[8] K. Y. Kim, A. J. Taylor, J. H. Glownia, and G. Rodriguez, "Coherent control of terahertz supercontinuum generation in ultrafast laser-gas interactions,", Nat. Photon. **2**, 605 (2008).

[9] T. D. Wang, Z.-M. Sheng, H.-C. Wu, M. Chen, C. Li, J. Zhang, and K. Mima, "Strong terahertz pulse generation by chirped laser pulses in tenuous gases," Opt. Express **16**, 16999 (2008).

[10] M. Chen, A. Pukhov, X.-Y. Peng, and O. Willi, "Theoretical analysis and simulations of strong terahertz radiation from the interaction of ultrashort laser pulses with gases," Phys. Rev. E **78**, 046406 (2008).

[11] K.-W. Kim, "Generation of coherent terahertz radiation in ultrafast laser-gas interactions," Phys. Plasma **16**, 056706 (2009).

[12] J. Dai, N. Karpowicz, and X.-C. Zhang, "Coherent Polarization Control of Terahertz Waves Generated from Two-Color Laser-Induced Gas Plasma," Phys. Rev. Lett. **103**, 023001 (2009).

[13] C. G. Durfee, A. R. Rundquist, S. Backus, C. Herne, M. H. Murnane, and H. C. Kapteyn, "Phase Matching of High-Order Harmonics in Hollow Waveguides," Phys. Rev. Lett. **83**, 2187 (1999).

[14] E. A. Gibson, A. Paul, N. Wagner, R. Tobey, D. Gaudiosi, S. Backus, I. P. Christov, A. Aquila, E. M. Gullikson, D. T. Attwood, M. M. Murnane, and H. C. Kapteyn, "Coherent soft x-ray generation in the water window with quasi-phase matching," Science, **302**, 95 (2003).

[15] P. Sprangle, J. R. Peñano, B. Hafizi, and C. A. Kapetanakos, "Ultrashort laser pulses and electromagnetic pulse generation in air and on dielectric surfaces," Phys. Rev. E **69**, 066415 (2004).

[16] L. Bergé, S. Skupin, R. Nuter, J. Kasparian and J.-P. Wolf, "Ultrashort filaments of light in weakly ionized, optically transparent media," Rep. Prog. Phys. **70**, 1633 (2007).

[17] L. D. Landau, and E. M. Lifshitz, *Quantum Mechanics* (Pergamon, New York, 1965), 2nd ed., p. 276.

[18] A. V. Husakou and J. Herrmann, "Supercontinuum Generation of Higher-Order Solitons by Fission in Photonic Crystal Fibers," Phys. Rev. Lett. **87**, 203901 (2001).

[19] P. Tzankov, O. Steinkellner, J. Zheng, M. Mero, W. Freyer, A. Husakou, I. Babushkin, J. Herrmann and Frank Noack, "High-power fifth-harmonic generation of femtosecond pulses in the vacuum ultraviolet using a Ti:sapphire laser," Opt. Express **15**, 6389 (2007).

[20] E. A. V. Markatili and R. A. Schmeltzer, "Hollow metallic and dielectric waveguides for long distance optical transmission and lasers," Bell Sys. Tech. J. **43** 1784 (1964).

[21] *Handbook of Optics*, ed. by M. Bass, McGraw-Hill, (1994).

[22] P. J. Leonard, "Refractive indices, Verdet constants and polarizabilities for inert gases," Atom. data nucl. data tables **14**, 21 (1974).

[23] W. M. Wood, C. W. Siders, and M. C. Downer, "Measurement of femtosecond ionization dynamics of atmospheric density gases by spectral blueshifting," Phys. Rev. Lett. **67**, 3523 (1991).

[24] S.C. Rae and K. Burnett, "Detailed simulations of plasma-induced spectral blueshifting," Phys. Rev. A **46**, 1084 (1992).

[25] I. Babushkin, W. Kuehn, C. Köhler, S. Skupin, L. Bergé, K. Reimann, M. Woerner, J. Herrmann, and T. Elsaesser, "Ultrafast spatio-temporal dynamics of terahertz generation by ionizing two-color femtosecond pulses in gases," in preparation.